Experimental and ab Initio Investigations of the Kinetics of the Reaction of H Atoms with H_2S

Jingping Peng, Xiaohua Hu, and Paul Marshall*

Department of Chemistry, University of North Texas, P.O. Box 305070, Denton, Texas 76203-5070

Received: October 23, 1998; In Final Form: April 12, 1999

The rate constant k_1 for the H + H_2S reaction has been measured from 298 to 598 K by the flash-photolysis resonance fluorescence technique, and the results are summarized as $k_1 = (6.6 \pm 0.9) \times 10^{-11} \exp[(-11.2 \pm 0.4)\ \text{kJ mol}^{-1}/RT]\ \text{cm}^3\ \text{molecule}^{-1}\ \text{s}^{-1}$ (1σ uncertainty in the parameters). The 95% confidence interval for k_1 is estimated as 20%. Combination with literature data reveals distinct curvature in the Arrhenius plot and a combined expression for 190−2237 K is $k_1 = 5.8^{+11.1}_{-3.8} \times 10^{-17}\ T^{1.94\pm0.15} \exp[(-455 \pm 67)/T]\ \text{cm}^3\ \text{molecule}^{-1}\ \text{s}^{-1}$. The geometry, frequencies, and energy of the transition state were investigated at up to the QCISD(T)/6-311+G(3df,2p) level of theory, and conventional transition state theory with Eckart tunneling corrections gave good accord with experiment up to about 1000 K. Neglect of variational effects appears to lead to errors of up to a factor of 2 at 2000 K.

1. Introduction

The reaction

$$H + H_2S \rightarrow H_2 + SH \qquad (1)$$

has been identified by Hynes and Wine as important in sulfur combustion under rich conditions.[1] An earlier review proposed a simple Arrhenius temperature dependence for the rate constant k_1,[2] but the recent measurements of Yoshimura et al. over 1053−2237 K and at 293 K were rationalized in terms of ab initio calculations and transition state theory (TST) with significant curvature in the Arrhenius plot.[3] The first aim of the present work was to provide new measurements of k_1 in the intermediate temperature regime, up to about 600 K. The second aim was to reexamine the transition state for this reaction at high levels of ab initio theory and to employ the results in conventional canonical TST. One aspect of the theoretical work was to see how reliable a nonvariational analysis would be for a reaction where the reaction barrier is modest.

2. Methodology

2.1. Experimental Technique. Detailed descriptions of the experimental apparatus and modifications for H-atom detection have been given elsewhere.[4−6] In this study, MgF_2 optics were employed. The atomic H was produced by pulsed photolysis of H_2S at 193 nm using a PSX-100 excimer laser (MPB Technologies). The relative concentration of H atoms was monitored using time-resolved resonance fluorescence at the Lyman-α wavelength (121.6 nm). The probing resonant radiation at 121.6 nm was generated by a microwave-excited discharge lamp (0.1% H_2 in Ar, 0.27 mbar). The reaction zone is defined as the intersection of the photolysis and probe beams. Fluorescence from the reaction zone was detected by a solar-blind photomultiplier tube (Hamamatsu, R1459) employed with pulse counting and signal averaging. The energy of the excimer laser pulses was measured with a pyroelectric detector (Molectron, J25LP). The laser beam was spread by a lens and passed through the reaction zone with a cross section of approximately $0.7 \times 0.7\ \text{cm}^2$. The temperature T of the gas in the reaction zone was measured before and after each set of k_{ps1} measurements with an unshielded thermocouple, corrected for radiation errors of up to 10 K, and is expected to be accurate to within ±2%.[7] All experiments were carried out in a large excess of Ar bath gas at a total pressure P. The H_2S concentrations were derived from P, T, the mole fraction of H_2S in the Ar mixture, and the flow rates of argon and the H_2S mixture.

Under pseudo-first-order conditions [H] ≪ [H_2S], the H atoms reacted with H_2S:

$$d[H]/dt = -(k_1[H_2S] + k_{diff})[H] = -k_{ps1}[H] \qquad (1)$$

where k_{diff} accounts for any loss of H atoms out of the reaction zone other than by reaction with H_2S, mainly via diffusion to the reactor walls. Typical values of k_{diff} were in the range of 100−450 s^{-1}. k_{ps1} was obtained by fitting the recorded fluorescence intensity I_f versus time profile to an exponential decay (an example is shown as the inset in Figure 1) over typically at least four lifetimes:

$$I_f = A \exp(-k_{ps1}t) + B \qquad (2)$$

The second-order H + H_2S rate constant k_1 was determined by linear fitting of k_{ps1} versus typically five values of [H_2S] (see Figure 1 for an example). To verify that pseudo-first-order conditions were maintained, the energy of the excimer laser beam was varied to alter the initial radical concentrations. The energy of the photolysis pulse (I_0, 0.1−0.6 mJ) was combined with the H_2S absorption cross section of about $8 \times 10^{-18}\ \text{cm}^2$ (base e, room temperature) at 193 nm[8] to estimate the initial concentrations $[H]_0$ and $[SH]_0$. Gas mixtures flowed through the reactor slowly compared to the reaction time scale of the H atoms, so the kinetic conditions were effectively static. The average gas residence time in the heated reactor before photolysis, τ_{res}, was varied by a factor of 2 or more to check for possible pyrolysis of H_2S.

2.2. Theoretical Calculations. The energies and harmonic vibrational frequencies of optimized structures for H, H_2, SH,

10.1021/jp984242l CCC: $18.00
Published on Web 06/11/1999

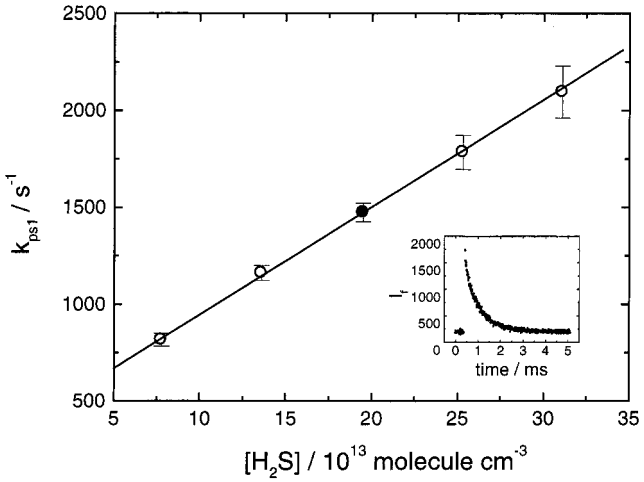

Figure 1. Plot of pseudo-first-order rate constant k_{ps1} vs [H_2S] at P = 33 mbar and T = 491 K. The inset shows the decay of time-resolved fluorescence intensity I_f for the solid point. The error bars are $\pm 2\sigma$.

H_2S, and the activated complex of reaction 1 were evaluated using the GAUSSIAN 94 program package[9] at the BHandH-LYP/6-311G(d,p), MP2/6-311G(d,p), QCISD/6-311G(d,p), and QCISD(T)/6-311+G(3df,2p) levels of theory.

Conventional TST was employed for the kinetic calculations, with the usual assumption of the separability of vibrational and rotational motions of the TS[10].

$$k_{TST} = \Gamma \frac{k_B T}{h} \frac{Q_{H_3S^{\ddagger}}}{Q_H Q_{H_2S}} \exp\left(-\frac{E_0^{\ddagger}}{RT}\right) \qquad (3)$$

where Γ is the Eckart correction factor for quantum mechanical tunneling.[10] The optimized geometries and vibrational frequencies at the QCISD(T)/6-311+G(3df,2p) level were used for evaluating Γ, the barrier to reaction including zero-point energy, $E_0^{\ddagger}$, and the partition functions Q. To allow for anharmonicity, the ab initio vibrational frequencies were multiplied by a scaling factor of 0.9552, which was obtained by plotting observed fundamentals for H_2S,[11] H_2[12], and SH[13] versus calculated frequencies.

3. Results

The experimental conditions and results for 41 k_1 measurements are summarized in Table 1.The listed 1σ uncertainties in k_1 are derived from the precision of slopes of plots such as Figure 1, combined in quadrature with the estimated reproducibility of P, T, and the gas flows. Modest values of σ/k_1 indicate good linearity in such plots, but the scatter between successive determinations of k_1 was significantly greater than can be accounted for by these σ values alone. At each temperature, we calculated the weighted and unweighted means plus the standard deviations of these means.[14] The two means at each temperature differ by up to 6%. The weighted mean and the larger of the two standard deviations at each temperature are reported in Table 1. Not all our original measurements are included in Table 1. Four outlying k_1 values were rejected according to Chauvenet's statistical criterion.[15] At 491 K, we also made measurements at short residence times, less than 0.75 s, but found these data as a group to be significantly smaller than the other measurements at 491 K. We therefore did not include these data in Table 1. Where the data at a given temperature do not overlap within the individual 2σ error bars,

TABLE 1: Measurements of the Rate Constants k_1 for the Reaction H + H_2S

T, K	P, mbar	τ_{res}, s	I_0, mJ	$[H]_{0,max}$, 10^{11} molecule cm^{-3}	$[H_2S]_{0,max}$[a], 10^{14} molecule cm^{-3}	$k_1 \pm \sigma_{k_1}$, 10^{-13} cm^{-3} molecule^{-1} s^{-1}
298	68.5	1.2	0.1	4.6	6.1	8.21 ± 0.14
299	200.4	1.2	0.1	4.6	6.0	8.15 ± 0.26
297	67.8	1.2	0.2	13.2	6.0	7.87 ± 0.17
297	67.0	1.1	0.2	13.1	6.0	7.98 ± 0.26
298	67.2	1.2	0.2	9.7	5.9	7.94 ± 0.20
298						8.05 ± 0.08[b]
337	67.0	2.0	0.2	44.6	20.5	9.93 ± 0.37
337	134.6	4.0	0.1	24.0	22.0	10.6 ± 0.22
338	134.3	2.0	0.1	22.7	20.9	9.57 ± 0.21
337	67.3	2.0	0.1	22.4	20.6	9.68 ± 0.15
337						9.88 ± 0.20[b]
386	67.2	0.8	0.2	9.2	4.2	16.3 ± 0.9
383	201.1	0.8	0.2	9.3	4.3	16.3 ± 0.3
386	66.7	0.8	0.1	4.6	4.2	18.9 ± 0.9
387	68.4	1.8	0.2	6.9	4.2	21.7 ± 0.8
386	69.2	3.6	0.2	9.2	5.6	24.4 ± 0.6
386	134.8	3.5	0.2	9.1	5.6	20.3 ± 1.2
386						18.6 ± 1.2[b]
432	66.3	1.5	0.1	4.6	4.3	27.8 ± 1.3
432	66.8	0.8	0.3	16.8	5.2	24.3 ± 0.9
432	66.8	0.8	0.1	5.6	5.2	20.5 ± 0.7
432	132.6	1.5	0.3	16.8	5.1	24.2 ± 2.1
432						22.9 ± 1.3[b]
490	66.4	2.0	0.3	12.9	4.0	30.5 ± 2.4
491	133.0	2.0	0.3	13.1	4.0	38.3 ± 1.3
491	34.5	2.3	0.2	9.7	4.5	64.6 ± 4.2
491	34.3	1.1	0.2	4.9	2.2	48.0 ± 3.3
491	33.9	2.2	0.2	6.9	3.2	42.4 ± 2.1
491	35.2	2.3	0.4	14.3	3.3	61.0 ± 1.3
491	34.1	1.1	0.4	8.1	1.9	48.0 ± 2.6
491	69.9	2.3	0.4	14.8	3.4	48.7 ± 0.8
491	69.8	2.3	0.2	5.6	3.4	50.3 ± 1.5
491	35.9	2.4	0.4	14.6	3.4	55.3 ± 1.1
491	35.9	2.4	0.1	3.6	3.4	58.8 ± 2.1
491						49.8 ± 2.9[b]
601	68.5	1.4	0.4	9.3	2.4	65.7 ± 9.0
598	34.5	1.8	0.6	16.6	2.5	56.6 ± 3.4
598	34.5	1.8	0.2	5.5	2.5	60.9 ± 3.4
598	68.1	1.8	0.6	16.9	2.6	60.2 ± 3.8
597	68.5	3.6	0.6	18.5	2.8	64.1 ± 1.6
598	68.7	1.2	0.6	17.5	2.7	68.6 ± 3.7
597	68.4	3.6	0.6	21.4	3.3	51.4 ± 1.7
598	35.2	1.9	0.5	16.5	3.0	54.5 ± 9.4
598	67.3	3.5	0.5	29.8	5.5	55.5 ± 4.8
599	67.3	1.8	0.5	29.9	5.5	56.7 ± 1.1
599	67.4	1.2	0.5	21.8	4.0	69.5 ± 4.3
598						58.4 ± 1.7[b]

[a] $[H_2S]_{0,max}$ was 2.3−6.3 times $[H_2S]_{0,min}$. [b] Weighted mean value ± rms deviation of the mean.

we checked for any systematic dependence of k_1 on five parameters: I_0, τ_{res}, $[H]_0$, $[H_2S]_0$, and P. Linear fits at each temperature were analyzed to see if the slope was significantly (at the 5% significance level) different from zero, via the correlation coefficient[16] (see the Supporting Information). In two cases, there appeared to be significant variation of k_1, at 386 K with τ_{res} and at 491 K with P. In both cases, the correlation depends on the inclusion of a single point at high pressure. The k_1 results were not dependent on $[H]_0$, which shows that secondary chemistry involving photolysis or reaction products was negligible within the range of laser energy used in this study and that pseudo-first-order conditions were attained. At the highest temperature, k_1 showed no consistent trend with τ_{res}, which indicates that pyrolysis of H_2S was unimportant at the listed temperatures.

To make an alternative estimate of the extent of interference from secondary chemistry, kinetic modeling was performed

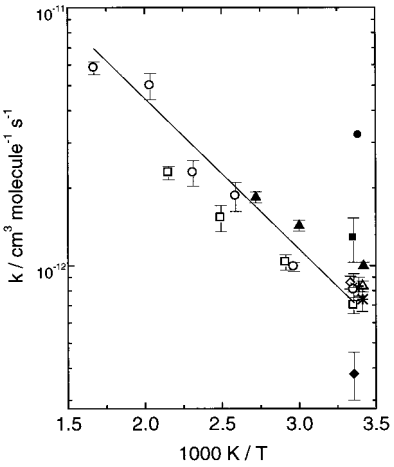

Figure 2. k_1 for the H + H_2S reaction in the range 293−600 K. (solid line) Arrhenius fitting of this work; (○) this work; (□) ref 19; (▲) ref 20; (△) ref 3; (◇) ref 21; (■) ref 22; (*) ref 23; (×) ref 24; (◆) ref 25; (+) ref 18; (●) ref 26. The error bars are $\pm 2\sigma$ if σ was given, otherwise, they are ± literature reported errors.

using the ACUCHEM program.[17] The following scheme was considered:

$$H + H_2S \rightarrow H_2 + SH,\ k_1 = 7.8 \times 10^{-13}\ cm^3\ molecule^{-1}\ s^{-1}$$

$$H + SH \rightarrow H_2 + S,\ k_2 = 2.2 \times 10^{-11}\ cm^3\ molecule^{-1}\ s^{-1}$$

$$S + SH \rightarrow H + S_2,\ k_3 = 5.0 \times 10^{-12}\ cm^3\ molecule^{-1}\ s^{-1}$$

$$SH + SH \rightarrow H_2S + S,\ k_4 = 3.2 \times 10^{-11}\ cm^3\ molecule^{-1}\ s^{-1}$$

$$H \rightarrow \text{diffusion},\ k_{diff} = 250\ s^{-1}$$

with the worst-case conditions $[H_2S]_0 = 6.0 \times 10^{14}$ molecule cm^{-3} and $[H]_0 = [SH]_0 = 1.3 \times 10^{12}$ molecule cm^{-3}. The value of k_1 was taken from this work and values of k_2, k_3, and k_4 were from Nicholas et al.[18] All are room-temperature values. For each modeling of a particular set of k_i values, linear regression was applied to the plot of ln[H] versus time. The resultant slope was $-k_{ps1}$ and the effective second-order rate constant was then estimated as $k_{eff} = (k_{ps1} - k_{diff})/[H_2S]_0$. The relative deviations of k_{eff} with respect to that without secondary chemistry ($k_2 = k_3 = k_4 = 0$) were 5.4% for the original k_i values, 8.7% for $k_3 = k_4 = 0$, and −1.4% for $k_2 = 0$. This reveals that the reaction H + SH → H_2 + S is the main source of interference. k_1 increases more rapidly with increasing temperature than k_2-k_4, so the primary reaction is more easily separated from any secondary chemistry at elevated temperatures. The energy of the photolyzing laser beam was employed as low as practicable in this work to minimize $[SH]_0$, and the ratio $k_1[H_2S]_0/k_2[SH]_0$ was maintained at 16 or larger.

A weighted Arrhenius fit was performed on the 41 measurements and is shown in Figure 2. It yielded

$$k_1 = (6.6 \pm 0.9) \times 10^{-11} \times \exp[(-11.2 \pm 0.4)\ kJ\ mol^{-1}/RT]\ cm^3\ molecule^{-1}\ s^{-1} \quad (4)$$

over the temperature range 298−598 K. The quoted errors in this expression are 1σ and are statistical only. Consideration of the covariance leads to a 1σ precision for the fitted k_1 of 3−6%, and allowance for possible systematic errors leads to 95% confidence intervals of ±20%.

In Table 2, are listed optimized geometries, barrier heights, and reaction enthalpies for the H + H_2S system calculated at the four different theory levels mentioned previously. The experimental values are listed for comparison also. The harmonic frequencies calculated at the corresponding optimized geometries together with measured harmonics and observed fundamentals are presented in Table 3.

The results of the TST calculation are shown in Figure 3. The dotted line represents a TST calculation adopting the QCISD(T)/6-311+G(3df,2p) barrier height of 16.0 kJ mol^{-1} and the corresponding Eckart corrections. The solid line represents a TST calculation adopting a barrier height of 14.4 kJ mol^{-1}, which was chosen to minimize the rms deviation from our experimental data. The reverse barrier height was varied also by the same amount as the reaction barrier height, and the imaginary frequency was unchanged when tunneling correction factors were calculated. The open circles are experimental data measured in this work.

Nonlinear fitting of the TST data calculated using $E_0^{\ddagger} = 14.4$ kJ mol^{-1} over 190−2237 K yields

$$k_1 = 1.68 \times 10^{-18}\ T^{2.44} \exp(-236/T)\ cm^3\ molecule^{-1}\ s^{-1} \quad (5)$$

This expression fits the TST data to within 10%.

4. Discussion

Figure 2 shows a comparison of the present results with earlier measurements[3,18−26] in the temperature range of our investigation. There is good accord with most of the room-temperature data, and at higher temperatures, our Arrhenius fit lies between the results of Kurylo et al.[19] and Mihelcic et al.[20] Figure 2 shows our results in comparison with two studies of $k_1(T)$ where T was varied substantially around room temperature,[19,20] together with high-temperature measurements.[3,27,28] Clearly, the higher the central temperature of the experiments, the larger the observed activation energy E_a. A fit to the present results (eq 4) together with the fit expressions from ref 3, 16, 17, and 24, evaluated at 10^{-4} K^{-1} intervals and weighted equally in ln k_1, yields the modified Arrhenius expression

$$k_1 = (5.8^{+11.1}_{-3.8} \times 10^{-17}) T^{1.94 \pm 0.15} \times \exp[(-455 \pm 67)/T]\ cm^3\ molecule^{-1}\ s^{-1} \quad (6)$$

which is a reasonable representation of the combined experimental data set, although it overestimates k_1 at 2237 K by about a factor of 1.5. The parameters of eq 6 agree to within the stated 1σ uncertainties with those of the analogous expression presented by Yoshimura et al.,[3] which overestimated k_1 at 2237 K by about a factor of 1.7. The common functional form $k = AT^n \exp(-B/T)$ may therefore not be the best expression for this rate constant, for which data are available over an unusually wide range of temperature.

Of the ab initio results in Table 2, our transition state geometry at MP2/6-311G(d,p) is the closest to the previous calculations by Yoshimura et al.[3] at the HF/6-31G(d,p) and MP2/6-31G(d,p) levels of theory. Our QCISD(T)/6-311+G(3df,2p) geometry is probably more accurate, based on the close accord with data for stable species where the bond lengths appear to be good to within about 10^{-12} m and the H_2S angle is in error by less than 0.1°, although the differences from the earlier geometry will have a negligible influence on $k_1(T)$.

It is noted that the calculated harmonic frequencies at the QCISD(T)/6-311+G(3df,2p) level for the stable species listed in Table 3 are in very good agreement with the measured values (relative deviations up to 0.4% and a rms deviation of 7 cm^{-1}).

TABLE 2: Geometry, Barrier Height, and Enthalpy for the Reaction H + H_2S

geometry[a], $E_0^{\ddagger}$, ΔH_0	BH and HLYP/ 6-311G(d,p)	MP2/ 6-311G(d,p)	QCISD/ 6-311G(d,p)	QCISD(T)/ 6-311+G(3df,2p)	exptl[c]
			H1···H2−S−H3 (TS)		
r(H1- -H2)	1.2385	1.055	1.1471	1.1613	
r(S−H2)	1.4046	1.4506	1.429	1.428	
r(S−H3)	1.3372	1.3356	1.3394	1.3411	
∠H1−H2−S	175.26	174.88	175.04	173.79	
∠H2−S−H3	92.27	90.32	90.78	90.85	
			H_2S		
r(S−H)	1.3361	1.3336	1.3377	1.3391	1.328
∠H−S−H	93.19	92.12	92.20	92.29	92.2
			H_2		
r(H−H)	0.7382	0.7384	0.7433	0.7422	0.7414
			SH		
r(S−H)	1.3405	1.3381	1.3429	1.3431	1.345
$E_0^{\ddagger}$, kJ mol^{-1}	10.72	32.26	21.95	16.00	
ΔH_0, kJ mol^{-1}	−67.82	−46.90	−64.99	−59.90	−61.96 ± 5.08 −55.90 ± 3.12[d]
scaling factor for ZPC[b]	0.9305	0.9244	0.9445	0.9552	

[a] Bond lengths in 10^{-10} m and angles in degrees. [b] Obtained by plotting observed frequencies vs calculated frequencies. [c] Taken from ref 13. [d] Obtained from ref 29.

TABLE 3: Harmonic Frequencies and Fundamentals for Species of the Reaction H + H_2S

modes[a]	BH and HLYP/ 6-311G(d,p)	MP2/ 6-311G(d,p)	QCISD/ 6-311G(d,p)	QCISD(T)/ 6-311+G(3df,2p)	measured harmonics[b]	fundamentals[b]
			Transition State			
A′	918i	1790i	1437i	1398i		
A′	420	516	464	459		
A′	483	596	526	522		
A′	1198	1149	1163	1166		
A′	1677	1391	1439	1455		
A′	2785	2811	2761	2748		
			H_2S			
A_1 (ν_2)	1257	1228	1231	1211	1215	1183
A_2 (ν_1)	2784	2817	2765	2711	2722	2615
B_2 (ν_3)	2797	2836	2781	2727	2733	2627
			H_2			
σ_g	4522	4533	4423	4411	4401	4159
			SH			
σ	2766	2796	2734	2690	2690	2599

[a] Designated in irreducible representations from ab initio calculations and in cm^{-1}. [b] Taken from refs 11−13.

The real frequencies of the transition state and H_2S do not vary strongly with the level of calculation, although they are generally slightly smaller than the earlier HF/6-31G(d,p) and MP2/6-31G(d,p) results.[3] These differences will have little impact on $k_1(T)$, but the imaginary frequency ν_i corresponding to motion along the reaction coordinate is important in determining the tunneling correction and is seen to vary significantly with the level of calculation. In particular, the earlier MP2/6-31G(d,p) value of 1890 cm^{-1} is greater than any found here. We would expect overestimation of the barrier height to correlate with overestimation of the curvature at the saddle point and hence ν_i; the close accord at the QCISD(T)/6-311+G(3df,2p) level between experiment and calculation for $E_0^{\ddagger}$ and ΔH_0 is therefore a necessary condition for an accurate assessment of ν_i.

The tunneling correction factor Γ increases from 1.04 at 2000 K through 4.1 at 298 K to about 27 at 190 K, so the TST results will be especially sensitive to details of the tunneling model at room temperature and below. Nevertheless, as shown in Figure 3, there is rather close accord with the experimental data in this region when the barrier is reduced by only 1.6 kJ mol^{-1} from the ab initio value. It is hard to say to what extent this correction reflects contributions from multidimensional tunneling paths, or simply residual energy errors at the QCISD(T)/6-311+G(3df,2p) level of theory, but in any event it is a modest correction to $E_0^{\ddagger}$. For comparison, Yoshimura obtained a PMP4/6-311G(d,p) barrier of 17.2 kJ mol^{-1}, adjusted to 13.4 kJ mol^{-1} to match experiment.[3]

Conventional TST calculations match experiment closely up to about 1000 K but overestimate k_1 above this temperature. For example, k_1 from eq 5 is a factor of 2.0 above the measurements of Yoshimura et al. at 2237 K, while the earlier TST calculations were a factor of 1.7 too large at this temperature.[3] A likely explanation is that variational effects become significant above 1000 K. In this case, that is where the average kinetic energy of the particles, 1.5RT, roughly equals the fitted barrier $E_0^{\ddagger}$ = 14.4 kJ mol^{-1}, but whether this is a general criterion for the need for nonvariational TST remains to be explored.

5. Conclusions

The rate constant for the H + H_2S reaction has been measured from 298 to 598 K, and the results coupled with a transition state theory analysis support the suggestion by Yoshimura et al. that the reaction shows significant curvature in the Arrhenius plot. With a 1.6 kJ mol^{-1} lowering of the reaction barrier from

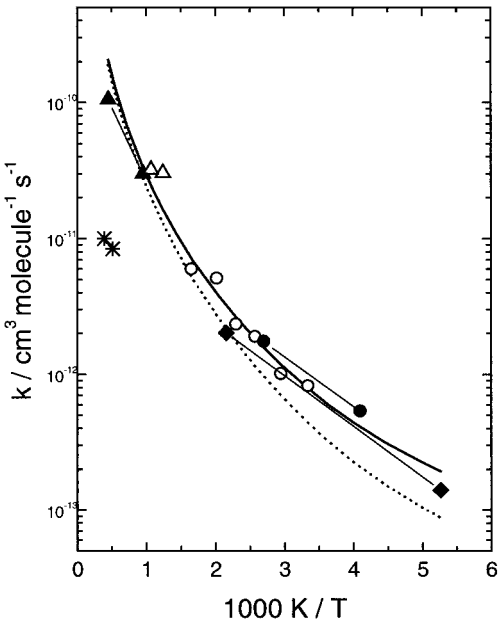

Figure 3. Comparison of k_1 value for the H + H_2S reaction. (○) this work; (- ◆ -) ref 19; (- ● -) ref 20; (- ▲ -) ref 3; (- * -) ref 28; (- △ -) ref 27; (dotted line) TST calculation with $E_0^{\ddagger} = 16.0$ kJ/mol; (solid line) TST calculation with $E_0^{\ddagger} = 14.4$ kJ/mol.

the QCISD(T)/6-311+G(3df,2p) value, conventional TST combined with an Eckart tunneling model accounts well for the observed rate constants over 190−1000 K. Above this temperature, nonvariational TST begins to overestimate the rate constant, by up to a factor of 2 at around 2000 K.

Acknowledgment. This work was supported by the Robert A. Welch Foundation (Grant B-1174) and the UNT Faculty Research Fund.

Supporting Information Available: Plots of k_1 versus experimental parameters at each temperature. This material is available free of charge via the Internet at http://pubs.acs.org.

References and Notes

(1) Hynes, A. J.; Wine, P. H. In *Combustion Chemistry*, 2nd ed.; Gardiner, W. C., Jr., Ed.; Chapter 3, in press.

(2) Baulch, D. L.; Drysdale, D. D.; Duxbury, J.; Grant, S. J. *Evaluated Kinetic Data for High-Temperature Reactions*; Butterworth: London, 1976; Vol. 3.

(3) Yoshimura, M.; Koshi, M.; Matsui, H.; Kamiya, K.; Umeyama, H. *Chem. Phys. Lett.* **1992**, *189*, 199.

(4) Shi, Y.; Marshall, P. *J. Phys. Chem.* **1991**, *95*, 1654.

(5) Ding, L.; Marshall, P. *J. Phys. Chem.* **1992**, *96*, 2197.

(6) Goumri, A.; Yuan, W.-J.; Ding, L.; Shi, Y.; Marshall, P. *Chem. Phys.* **1993**, *177*, 233.

(7) Ding, L.; Marshall, P. *J. Chem. Soc., Faraday Trans.* **1993**, *89*, 419.

(8) Okabe, H. In *Photochemistry of Small Molecules*; John Wiley: New York, 1978; p 204.

(9) Frisch, M. J.; Trucks, G. W.; Schlegel, H. B.; Gill, P. M. W.; Johnson, B. G.; Robb, M. A.; Cheeseman, J. R.; Keith, T. A.; Petersson, G. A.; Montgomery, J. A.; Raghavachari, K.; Al-Laham, M. A.; Zakrzewski, V. G.; Ortiz, J. V.; Foresman, J. B.; Cioslowski, J.; Stefanov, B. B.; Nanayakkara, A.; Challacombe, M.; Peng, C. Y.; Ayala, P. Y.; Chen, W.; Wong, W.; Andres, J. L.; Replogle, E. S.; Gomperts, R.; Martin, R. L.; Fox, D. J.; Binkley, J. S.; Defrees, D. J.; Baker, J.; Stewart, J. P.; Head-Gordon, M.; Gonzalez, C.; Pople, J. A. *Gaussian 94*, revision D.2; Gaussian, Inc.: Pittsburgh, PA, 1995.

(10) Johnston, H. S. *Gas-Phase Reaction Rate Theory*; Ronald: New York, 1966.

(11) Allen, H. C.; Plyler, E. K. *J. Chem. Phys.* **1956**, *25*, 1132.

(12) Huber, K. P.; Herzberg, G. *Constants of Diatomic Molecules*; Van Nostrand Reinhold: New York, 1979; Vol. 4.

(13) Chase, M. W., Jr.; Davies, C. A.; Downey, J. R., Jr.; Frurip, D. J.; McDonald, R. A.; Syverud, A. N. *J. Phys. Chem. Ref. Data* **1985**, *14* (Suppl. 1), JANAF Thermochemical Tables (3rd ed.).

(14) Massey, B. S. *Measures in Science and Engineering: Their Expression, Relation and Interpretation*; John Wiley: New York, 1986; p 87.

(15) Pugh, E. M.; Winslow, G. H. *The Analysis of Physical Measurements*; Addison-Wesley: Reading, 1966; p 109.

(16) Kleinbaum, D. G.; Kupper, L. L.; Muller, K. E.; Nizam, A. *Applied Regression Analysis and Other Multivariable Methods*; Duxbury Press: Pacific Grove, 1998; pp 24, 55, 96.

(17) Braun, W.; Herron, J. T.; Kahaner, D. K. *Int. J. Chem. Kinet.* **1988**, *22*, 51.

(18) Nicholas, J. E.; Amodio, C. A.; Baker, M. J. *J. Chem. Soc., Faraday Trans. 1* **1979**, *75*, 1868.

(19) Kurylo, M. J.; Peterson, N. C.; Braun, W. *J. Chem. Phys.* **1970**, *54*, 943.

(20) Mihelcic, D.; Schindler, R. N. *Ber. Bunsen-Ges. Phys. Chem.* **1970**, *74*, 1280.

(21) Husain, D.; Slater, N. K. H. *J. Chem. Soc., Faraday Trans. 2* **1980**, *76*, 276.

(22) Perner, D.; Franken, T. *Ber. Bunsen-Ges. Phys. Chem.* **1969**, *73*, 897.

(23) Clyne, M. A. A.; Ono, Y. *Chem. Phys. Lett.* **1983**, *94*, 597.

(24) Bradley, J. N.; Trueman, S. P.; Whytock, D. A.; Zaleski, T. A. *J. Chem. Soc., Faraday Trans. 1* **1973**, *69*, 416.

(25) Rommel, H.; Schiff, H. I. *Int. J. Chem. Kinet.* **1972**, *4*, 547.

(26) Cupitt, L. T.; Glass, G. P. *Trans. Faraday Soc.* **1970**, *66*, 3007.

(27) Pratt, G.; Rogers, D. *J. Chem. Soc., Faraday Trans. 1* **1977**, *73*, 54.

(28) Roth, P.; Lohr, R.; Barner, U. *Combust. Flame* **1982**, *45*, 273.

(29) Nicovich, J. M.; Kreutter, K. D.; van Dijk, C. A.; Wine, P. H. *J. Phys. Chem.* **1992**, *96*, 2518.